J. Fluid Mech. (1987), *vol.* 178, *pp.* 279–302
Printed in Great Britain

On the reflection of a train of finite-amplitude internal waves from a uniform slope

By S. A. THORPE†
With an appendix by
S. A. THORPE AND A. P. HAINES
Institute of Oceanographic Sciences, Wormley, Godalming, Surrey, UK

(Received 7 April 1986 and in revised form 3 October 1986)

The reflection of a train of two-dimensional finite-amplitude internal waves propagating at an angle β to the horizontal in an inviscid fluid of constant buoyancy frequency and incident on a uniform slope of inclination α is examined, specifically when $\beta > \alpha$. Expressions for the stream function and density perturbation are derived to third order by a standard iterative process. Exact solutions of the equations of motion are chosen for the incident and reflected first-order waves. Whilst these individually generate no harmonics, their interaction does force additional components. In addition to the singularity at $\alpha = \beta$ when the reflected wave propagates in a direction parallel to the slope, singularities occur for values of α and β at which the incident-wave and reflected-wave components are in resonance; strong nonlinearity is found at adjacent values of α and β. When the waves are travelling in a vertical plane normal to the slope, resonance is possible at second order only for $\alpha < 8.4°$ and $\beta < 30°$. At third order the incident wave is itself modified by interaction with reflected components. Third-order resonances are only possible for $\alpha < 11.8°$ and, at a given α, the width of the β-domain in which nonlinearities connected to these resonances is important is much less than at second order. The effect of nonlinearity is to reduce the steepness of the incident wave at which the vertical density gradient in the wave field first becomes zero, and to promote local regions of low static stability remote from the slope. The importance of nonlinearity in the boundary reflection of oceanic internal waves is discussed.

In an Appendix some results of an experimental study of internal waves are described. The boundary layer on the slope is found to have a three-dimensional structure.

1. Introduction

It has not, as yet, proved possible to account satisfactorily for the mid-depth ocean diapycnal diffusivity of about 1 $cm^2\ s^{-1}$ required by the global budget calculations of Munk (1966); see Garrett (1979). Recently however Eriksen (1985) has drawn attention to a possible contribution resulting from the reflection of internal gravity waves at sloping ocean boundaries. He suggests that their transformation in wavenumber space and the enhanced energy flux which can occur at certain frequencies, may lead to wave breaking and hence to a generation of turbulence sufficient to account for much of the diffusion which must occur at mid-depth.

Eriksen's argument rests on both estimates and observations. The former are based on a *linear* theory of wave reflection which predicts the modification to an ambient

† Present address: Department of Oceanography, The University, Southampton SO9 5NH, UK.

wave spectrum by the reflection of component waves at a sloping boundary. A distorted spectrum results. It is however observed (Eriksen 1982) that beyond a few hundred metres from sloping topography, the internal-wave spectrum has approximately a universal form independent of position; anomalies are found only close to slopes. Eriksen argues that some of the energy flux from the distorted spectrum must be dissipated close to the boundary by wave breaking, and he points out that only a small fraction of the flux involved in this adjustment needs be used in diapycnal mixing to account for the canonical Munk estimate.

Precise calculation of the effects of the reflection process is however hampered by the lack of knowledge of the conditions which favour wave breaking and the efficiency of breaking in transferring kinetic to potential energy (Thorpe 1987), and particularly of the nonlinear consequences of internal-wave reflection. It is this nonlinear aspect which we address here in the hope of understanding more clearly the conditions which may favour wave breaking. For simplicity we focus attention primarily on a two-dimensional wavetrain in a non-rotating semi-infinite fluid of uniform density gradient with motion in a vertical plane normal to an infinite inclined plane boundary, this being a simple point of departure for a more detailed investigation. The linear reflection was discussed by Phillips (1966). Subsequent analytical and experimental work, principally by Wunsch and Cacchione, will be described when reference is appropriate. Some additional laboratory experiments have been made in connection with the present study, and these are described in Appendix C.

2. Analysis

2.1. *Properties of an exact solution for a progressive wavetrain*

The reflection of a monochromatic (i.e. single-frequency) train of two-dimensional internal gravity waves in an inviscid non-rotating incompressible Boussinesq fluid of constant density gradient from a uniform slope normal to their plane of motion may be characterized by three parameters. These are

(i) the angle between the slope and the horizontal α,

(ii) the angle between the incident wave group velocity and the horizontal β, and

(iii) a measure of the steepness of the incident waves s.

The angle β is given by

$$\sin\beta = \frac{\sigma}{N_0}, \tag{1}$$

(Phillips 1966), where σ is the incident-wave frequency and N_0 is the constant mean buoyancy frequency of the fluid. The ratio of the horizontal and vertical wavenumbers of this incident wavetrain, k and n respectively, is given by

$$\frac{k^2}{n^2} = \frac{\sigma^2}{N_0^2-\sigma^2} = \tan^2\beta. \tag{2}$$

The stream function

$$\psi = a\sin(kx+nz-\sigma t), \tag{3}$$

and density perturbation

$$\rho = \rho_0 \frac{N_0^2}{g}\frac{ak}{\sigma}\sin(kx+nz-\sigma t), \tag{4}$$

to the density field $\rho_0(1-N_0^2 z/g)$, is an exact solution of the full nonlinear equations of motion describing a train of freely propagating waves. Here ρ_0 is a reference density, g is the acceleration due to gravity and x, z are horizontal and vertically

upward axes respectively. The displacements of density surfaces from the reference density $\rho_0(1-N_0^2 z/g)$ is $\zeta(x,z,t)$ where

$$\zeta = \frac{ak}{\sigma}\sin(kx+n(z+\zeta)-\sigma t) \tag{5}$$

and $\max(\zeta) = ak/\sigma = A$ is the wave amplitude. It follows that even though the stream function is sinusoidal, isopycnal displacements at finite amplitude are asymmetrical. The isopycnal slope found by differentiating (5) is

$$\frac{\partial\zeta}{\partial x} = \frac{Ak\cos(kx+n(z+\zeta)-\sigma t}{1-An\cos(kx+n(z+\zeta)-\sigma t)}.$$

Static instability occurs when the local buoyancy frequency N given by

$$N^2 = N_0^2 - \frac{g}{\rho_0}\frac{\partial\rho}{\partial z} = N_0^2[1-An\cos(kx+nz-\sigma t)] \tag{6}$$

becomes negative, that is when $An > 1$. It is thus natural to characterize the wave steepness by $s = An$, so that the maximum wave slope is $s\tan\beta/(1-s)$ if $s < 1$ or is infinite if $s \geqslant 1$. (It is pertinent to note that the local Richardson number,

$$Ri = N^2/(\partial^2\psi/\partial z^2)^2,$$

is given by

$$Ri = \frac{1}{s^2\cos^2\beta}\frac{(1-sy)}{(1-y^2)}, \tag{7}$$

where $y = \cos(kx+nz-\sigma t)$ and, for $0 < s \leqslant 1$, $J = \min(Ri)$ is given by

$$J = \frac{1}{2\cos^2(1-N(1-\sigma^2))}, \tag{8}$$

which is $\geqslant \frac{1}{2}$, so that even in a slowly varying flow where it might be applicable, the Miles–Howard necessary conditions for instability, $J < \frac{1}{4}$, cannot be achieved.)

The stability of the finite-amplitude wavetrain to parametric disturbances has been considered by Mied (1976). In what follows we shall assume that the incident wavetrain is itself stable in the absence of reflection or, if unstable, becomes so only on a timescale much in excess of that involved in the process of reflection.

2.2. *Linear reflection*

We have chosen to consider a wave given by (3) and (4) incident on a slope of angle α. It is convenient to transfer axes x' and z' located up the line of greatest slope and normal to the slope (figure 1), and to take wavenumbers k', n' measured relative to the new coordinates. The fluid reference density is now $\rho_0[(1-N_0^2(z'c_\alpha+x's_\alpha)/g)]$ where s_α, c_α are $\sin\alpha$ and $\cos\alpha$ respectively and the wavenumbers are related by

$$k = k'c_\alpha - n's_\alpha, \quad n = k's_\alpha + n'c_\alpha. \tag{9}$$

Dropping the superscripts, the equations for the incident waves, (3) and (4) become

$$\psi = a\sin(kx+nz-\sigma t) \tag{10}$$

and

$$\rho = \frac{N_0^2}{g\sigma}a(kc_\alpha - ns_\alpha)\sin(kx+nz-\sigma t), \tag{11}$$

where here, and later, we have normalized ρ by dividing by ρ_0.

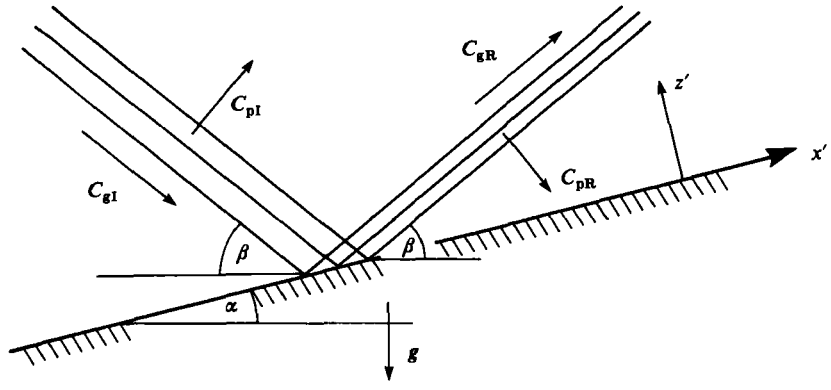

FIGURE 1. Sketch showing the incident (subscript I) and reflected (subscript R) first-order waves and their phase (C_p) and group (C_g) velocities.

The dispersion relation becomes

$$\frac{\sigma^2}{N_0^2} = \frac{(kc_\alpha - ns_\alpha)^2}{k^2+n^2} = s_\beta^2 \tag{12}$$

(where $s_\beta = \sin\beta$), which has two roots for n,

$$n_I = \frac{k}{2\gamma}(\sin 2\beta - \sin 2\alpha) \tag{13}$$

and

$$n_R = -\frac{k}{2\gamma}(\sin 2\beta + \sin 2\alpha), \tag{14}$$

where $\gamma = s_\beta^2 - s_\alpha^2$.

Recalling the relation between the directions of the group velocity and phase velocity for internal waves (Görtler 1943; Mowbray & Rarity 1967; see figure 1), we see that a wave with positive n has a downward group velocity, towards the slope. For the purposes of illustration and to be definite in ascribing signs, we suppose that $\beta > \alpha$ and $k > 0$. Then n_I is positive and n_R negative. We ascribe n_I to the incident wave, and the principal reflection is then up the slope as illustrated in figure 1. (If $\beta < \alpha$ the incident wave is reflected downslope.)

The boundary condition on the slope is that there is no normal velocity;

$$\frac{\partial\psi}{\partial x} = 0 \quad \text{at } z = 0. \tag{15}$$

The equations of motion can be written as vorticity

$$\frac{\partial}{\partial t}\nabla^2\psi - g\left(c_\alpha\frac{\partial}{\partial x} - s_\alpha\frac{\partial}{\partial z}\right)\rho = \left(\frac{\partial\psi}{\partial x}\frac{\partial}{\partial z} - \frac{\partial\psi}{\partial z}\frac{\partial}{\partial x}\right)\nabla^2\psi; \tag{16}$$

and conservation of density

$$\frac{\partial\rho}{\partial t} + \frac{N_0^2}{g}\left(c_\alpha\frac{\partial}{\partial x} - s_\alpha\frac{\partial}{\partial z}\right)\psi = \left(\frac{\partial\psi}{\partial x}\frac{\partial}{\partial z} - \frac{\partial\psi}{\partial z}\frac{\partial}{\partial x}\right)\rho; \tag{17}$$

which can be combined as

$$\left[\frac{\partial^2}{\partial t^2}\nabla^2+N_0^2\left(c_\alpha\frac{\partial}{\partial x}-s_\alpha\frac{\partial}{\partial z}\right)^2\right]\psi=\frac{\partial}{\partial t}\left(\frac{\partial\psi}{\partial x}\frac{\partial}{\partial z}-\frac{\partial\psi}{\partial z}\frac{\partial}{\partial x}\right)\nabla^2\psi$$
$$+\left(c_\alpha\frac{\partial}{\partial x}-s_\alpha\frac{\partial}{\partial z}\right)\left[\left(\frac{\partial\psi}{\partial x}\frac{\partial}{\partial z}-\frac{\partial\psi}{\partial z}\frac{\partial}{\partial x}\right)\rho\right]. \quad (18)$$

The stream function (10) and density (11) satisfy these equations exactly when n is given by (13) or (14), and the difference of these exact solutions,

$$\psi_1=a[\sin(kx+n_{\mathrm{I}}z-\sigma t)-\sin(kx+n_{\mathrm{R}}z-\sigma t)], \quad (19)$$

$$\rho_1=\frac{N_0^2a}{g\sigma}[(kc_\alpha-n_{\mathrm{I}}s_\alpha)\sin(kx+n_{\mathrm{I}}z-\sigma t)-(kc_\alpha-n_{\mathrm{R}}s_\alpha)\sin(kx+n_{\mathrm{R}}z-\sigma t)], \quad (20)$$

satisfies the boundary condition (15). This is the linear solution, essentially that proposed by Phillips (1966).

The singularity in n_{R} when $\alpha=\beta$ ($\gamma=0$) when the reflected waves are directed parallel to the slope has been discussed by Wunsch (1969) and Eriksen (1985). The non-dimensional density gradient N^2/N_0^2 is bounded below by $1-A\{|ks_\alpha+n_{\mathrm{I}}c_\alpha|+|ks_\alpha+n_{\mathrm{R}}c_\alpha|\}$ and the steepness of the incident wave is $s=A(ks_\alpha+n_{\mathrm{I}}c_\alpha)$, or, using (13), $Akc_\beta\sin(\beta-\alpha)/\gamma$.

2.3. *Higher-order solutions*

Although the incident and reflected linear waves individually satisfy (16)–(18), interaction between these waves occurs through the terms on the right-hand side of the equations. We now set up an iterative method of solution, regarding ψ_1 and ρ_1 as being the first-order approximation, and successively generating higher-order terms, $\psi_2,\psi_3,\ldots$, in $\psi=\Sigma\psi_i$ by solution of (18) together with the boundary condition (15), and in $\rho(\rho_2,\rho_3,\ldots)$ by solution of (16) and (17) selecting, where appropriate, solutions representing waves which radiate their energy away from the boundary.

At second order the product terms on the right-hand side of (18) produce contributions to ψ with coefficients containing a^2 (a may be regarded as an ordering parameter) and sinusoidal in $(2kx+(n_{\mathrm{I}}+n_{\mathrm{R}})z-2\sigma t)$ and $(n_{\mathrm{I}}-n_{\mathrm{R}})z$ (see table 1). The *latter* term provides a steady Eulerian flow parallel to the slope but which is found to be zero in a Lagrangian framework (as it must to preserve the density field – there is no diffusion in this formulation, unlike the studies of Phillips 1970, and Wunsch 1970 in which currents are induced by diffusion), together with a perturbation to the density field corresponding to a set-up of the isopycnal surfaces (see also Wunsch 1971). The *former* term may be a free wave if vector wavenumber and frequency $(2k,n_{\mathrm{I}}+n_{\mathrm{R}},2\sigma)$ satisfy the dispersion relation (12), in which case the incident and reflected waves will interact resonantly with the forced second-order mode. This is possible only for sufficiently small α, less than 8.4° (see figure 2).

Resonance only occurs for particular wavenumber–frequency combinations described below and, in general, to satisfy the boundary condition (15), it is necessary to introduce the free wave $(2k,m_2,2\sigma)$ which satisfies the dispersion relation and which radiates away from the boundary;

$$m_2=-\frac{2k[s_\alpha c_\alpha+2s_\beta(1-4s_\beta^2)^{\frac{1}{2}}]}{4s_\beta^2-s_\beta^2}. \quad (21)$$

x-wavenumber	z-wavenumber	Frequency	Comments
First-order components			
k	n_I	σ	Incident wave
k	n_R	σ	'Free wave'
Second-order components			
$2k$	n_I+n_R	2σ	Forced wave; may form one of resonant triad with first-order pair (figure 2)
0	n_I-n_R	0	Steady flow parallel to slope
$2k$ (N.B. no $(2k, 2n, 2\sigma)$ terms)	m_2	2σ	Required to satisfy b.c. at $z=0$. Free wave if $2\sigma < N_0$. Evanescent if $2\sigma > N_0$ ($\beta > 30°$)
Third-order components			
$3k$	$2n_I+n_R$	3σ	May form resonant triad with first-order incident and second-order forced wave (figure 5)
$3k$	$2n_R+n_I$	3σ	No resonance possible
k	$2n_I-n_R$	σ	
k	$2n_R-n_I$	σ	
$3k$	m_2+n_I	3σ	May form resonant triad with first-order incident and second-order free wave (figure 6)
$3k$	m_2+n_R	3σ	No resonance possible
k	m_2-n_I	σ	Resonant at second-order resonance
k	m_2-n_R	σ	No resonance possible
k	n_I	σ	Forces a modification to n_I (if k, σ are held constant)
k	n_R	σ	(i) n_R modified (ii) component required to satisfy b.c.
$3k$	m_3	3σ	Required to satisfy b.c. at $z=0$. Free wave if $3\sigma < N_0$. Evanescent if $3\sigma > N_0$ ($\beta > 19.47°$)

TABLE 1. Sequence of wave components up to third order

This wave mode is evanescent when $4s_\beta^2 > 1$, that is when $\beta > \frac{1}{6}$ or $2\sigma > N_0$, and is an exact solution of the equations (16)–(18). The forced wave $(2\sigma, n_I+n_R, 2\sigma)$ is not an exact solution and will develop its own harmonics at higher even orders.

The second-order solution is given in Appendix A, together with expressions for the mean Eulerian flow, the set-up of isopycnal surfaces and the apparent density flux resulting from wave reflection. In the (singular) limit $\alpha = 0$, there is no interaction between the first-order waves, and no Eulerian flow, although in this case there *is* a (horizontal) Lagrangian flow (see Thorpe 1968). As an example, figure 3 shows the waves at second order for $\alpha = 20°$, $\beta = 37.9°$ and $s = 0.070$. (The values are chosen for later comparison with experiment; see Appendix C.) These values of α and β are remote from possible resonance (figure 2). The solutions are dominated

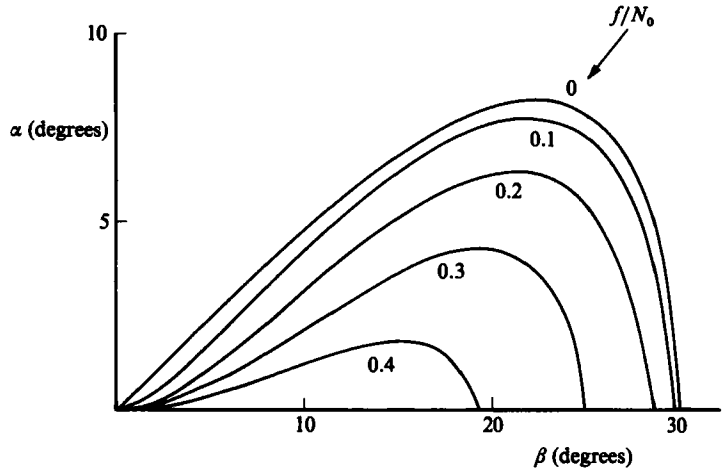

FIGURE 2. The loci of points in the (α, β)-plane where conditions of resonance are found at second order. The effect of variation in the parameter f/N_0 where f is the local inertial frequency are shown.

by the large-amplitude reflected first-order wave, and the second-order contributions are small even though the steepness of the composite reflected and incident waves is large. The conditions of second-order resonance (and hence values of α and β at which second-order terms are likely to be very important) when the incident wavetrain propagates with a component along the slope, are considered in Appendix B. The angles α at which resonance occurs for a given β increases as the along-slope wavenumber increases.

At higher orders there is a proliferation of terms which are harmonics in x and t and with z-wavenumbers which are sums and differences of n_{I}, n_{R} and m_2 or integer multiples of these terms, together with additional 'free waves' $(jk, m_j, j\sigma)$, $j = 3, 4, \ldots$, where m_j is given by

$$\mathscr{F}(l, m, \Sigma) \equiv \Sigma^2(l^2+m^2) - N_0^2(lc_\alpha - ms_\alpha)^2 = 0, \tag{22}$$

with $l = jk$, $m = m_j$ and $\Sigma = j\sigma$. The terms generated at third order are summarized in table 1. Products of the second-order $(2k, n_{\mathrm{I}}+n_{\mathrm{R}}, 2\sigma)$ and first-order $(k, n_{\mathrm{I}}$ or $n_{\mathrm{R}}, \sigma)$ wave terms lead to the generation of terms on the right-hand side of (18) with vector wavenumber and frequency (k, n_{R} or n_{I}, and σ) identical with those of the first-order waves; in the field of the reflected waves it is no longer possible to retain the form of the incident wave with the exact solution (3). We suppose, to be specific, that the wavenumber parallel to the slope and the frequency of the incident wave are prescribed as, for example, they might be in an experiment in which a wave-maker is aligned parallel to the slope producing periodic and sinusoidal waves along its length but absorbing all reflected waves. For the terms in question, (18) becomes

$$\frac{\partial^2}{\partial t^2}\nabla^2\psi_{31} + N_0^2\left(c_\alpha\frac{\partial}{\partial x} - s_\alpha\frac{\partial}{\partial z}\right)^2\psi_{31} = \Phi[\sin(kx+n_{\mathrm{I}}z-\sigma t) - \sin(kx+n_{\mathrm{R}}-\sigma t)], \tag{23}$$

when $\beta \leqslant 30°$, where $\Phi = 4a^3k^6s_\beta^2c_\beta^4(1-4s_\beta^2)/(\gamma^2 D)$ and D is given in Appendix A. ($D = 0$ is the condition for second-order resonance.) We now suppose that n_{I} and n_{R}, like ψ, can be expanded; $n_{\mathrm{I}} = n_{\mathrm{I}1} + n_{\mathrm{I}2} + \ldots$ (similarly n_{R}), where $n_{\mathrm{I}1}$, $n_{\mathrm{R}1}$ are given by (13) and (14) respectively, and the terms are successively ordered with powers of

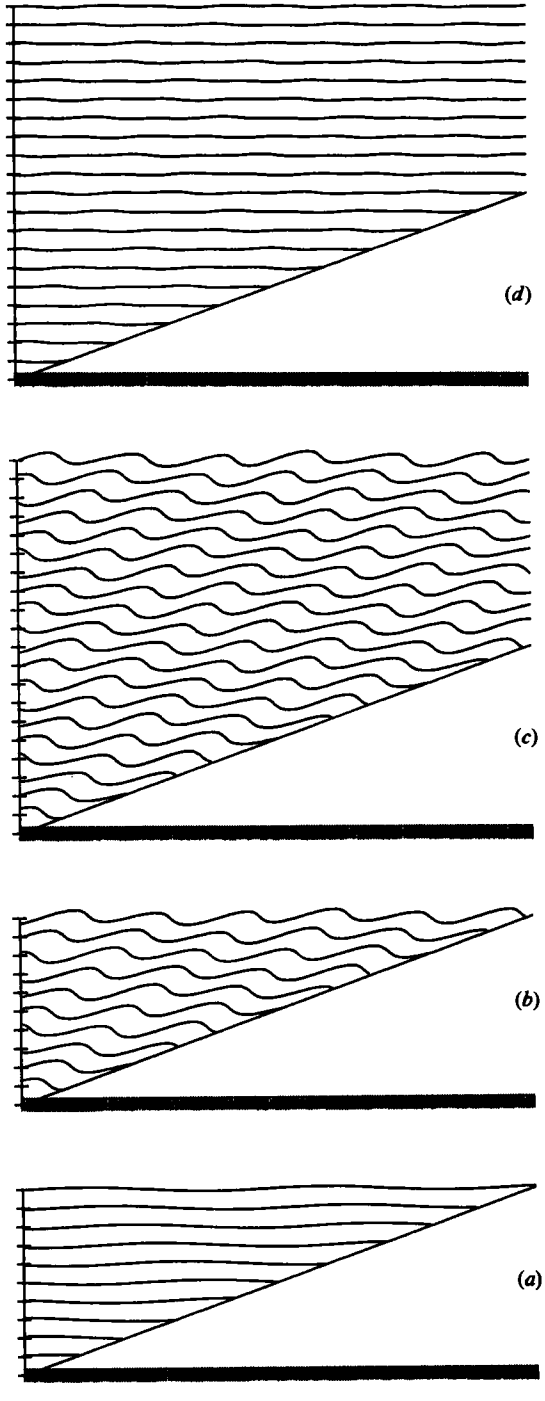

FIGURE 3. Wave reflection when $\alpha = 20°$, $\beta = 37.9°$ and $s = 0.070$. (*a*) shows the incident waves, (*b*) the incident and reflected wave at first order, (*c*) the incident and reflected waves, including the second-order terms which are shown in (*d*).

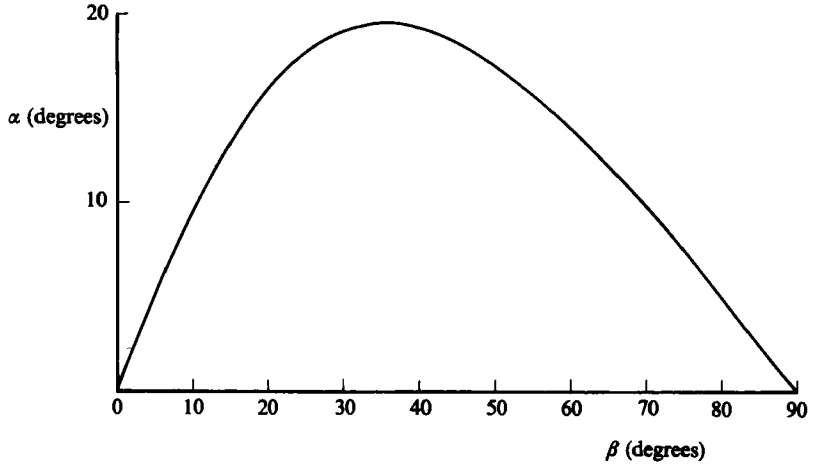

FIGURE 4. The locus of points in the (α, β)-plane at which a second-order correction to the wave number n_{I} is appropriate (see (26)).

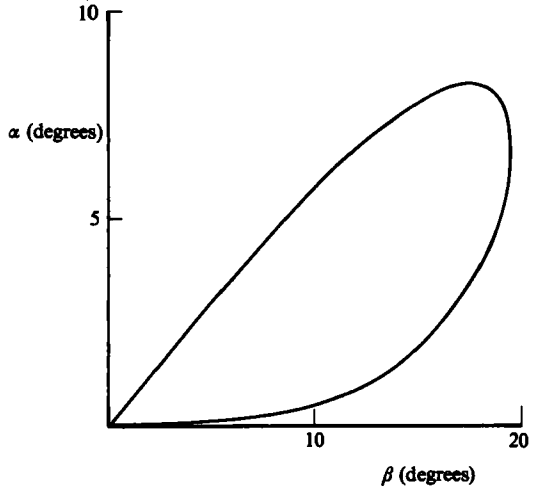

FIGURE 5. The locus of points in the (α, β)-plane for which the third-order $(3k, 2n_{\mathrm{I}}+n_{\mathrm{R}}, 3\sigma)$ wave is resonant.

a. Then substituting (19) into (23) and equating coefficients to order a^2, a^3 we find that $n_{\mathrm{I}2} = n_{\mathrm{R}2} = 0$ and

$$n_{\mathrm{I}3} = \frac{\Phi}{2\sigma^2 a[n_{\mathrm{I}1}\, s_\beta^2 - s_\alpha^2(kc_\alpha - n_{\mathrm{I}1}\, s_\alpha)^2]}, \tag{24}$$

$$n_{\mathrm{R}3} = \frac{\Phi}{2\sigma^2 a[n_{\mathrm{R}1}\, s_\beta^2 - s_\alpha^2(kc_\alpha - n_{\mathrm{R}1}\, s_\alpha)^2]}. \tag{25}$$

The denominator in (25) is non-zero. However, that of $n_{\mathrm{I}3}$ is zero when

$$s_\alpha^2 = \frac{s_\beta^2(1-s_\beta^2)}{1+3s_\beta^2}, \tag{26}$$

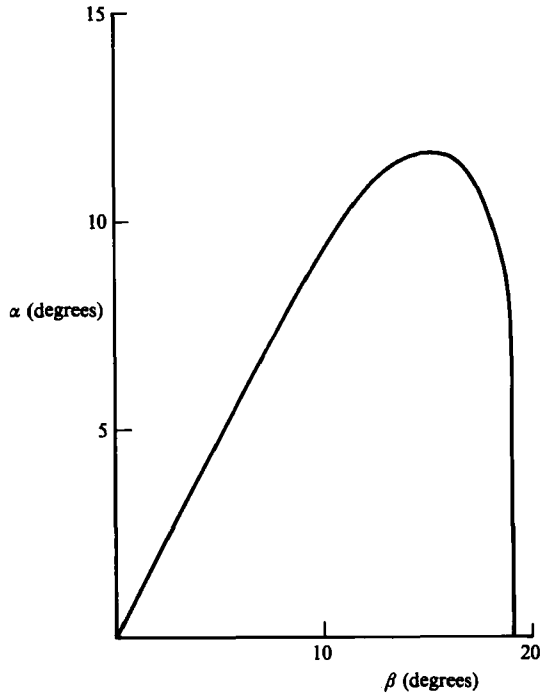

FIGURE 6. The locus of points in the (α, β)-plane for which the third-order $(3k, n_{\mathrm{I}}+m_3, 3\sigma)$ wave is resonant.

(see figure 4) and at these values we find

$$n_{\mathrm{I}2} = \frac{s_\beta \Phi^{\frac{1}{2}}}{\sigma(a\gamma)^{\frac{1}{2}}}, \tag{27}$$

(Φ is positive when (26) is satisfied).

As at second order, the boundary condition (15) at $z = 0$ is satisfied by introducing radiating free modes. The terms of slope wavenumber k and frequency σ are catered for by adding terms in a^3 to the coefficient of the linear radiating waves $(k, n_{\mathrm{R}1}, \sigma)$, whilst those of wavenumber $3k$ and frequency 3σ are matched by a wave $(3k, m_3, 3\sigma)$ with m_3 being the negative root of (22):

$$m_3 = -\frac{3k[s_\alpha c_\alpha + 3s_\beta(1-9s_\beta^2)^{\frac{1}{2}}]}{9s_\beta^2 - s_\alpha^2}. \tag{28}$$

This wave is evanescent if $s_\beta > \frac{1}{3}$ ($\beta > 19.4°$ or $3\sigma > N_0$).

Resonances possible between first-, second- and third-order waves are noted in table 1 and the (α, β)-curves on which they occur are shown in figures 5 and 6. Third-order resonances are only possible for $\alpha < 11.8°$, the largest value of α in the resonance curve of figure 6. The full third-order solutions for $\beta \leqslant \sin^{-1}(\frac{1}{3})$ are given in Appendix A.

3. Discussion

As table 1 shows, the effect of increasing the order of the solution is rapidly to generate more terms. The ratios of the z-wavenumbers of these terms are, in general, irrational numbers so that the wavefield becomes more disordered with energy being

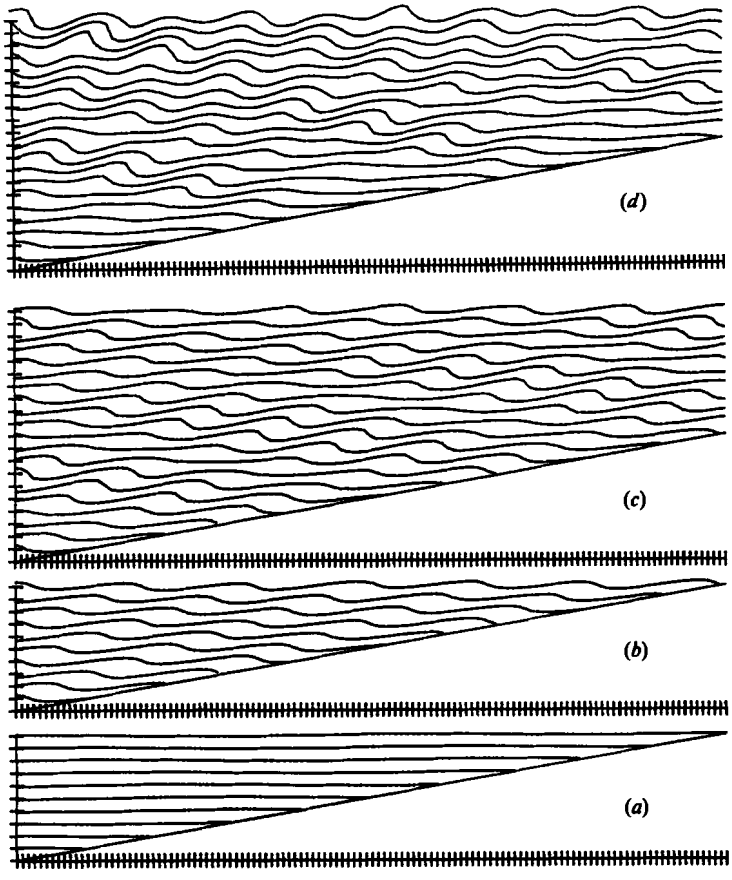

FIGURE 7. Wave reflection when $\alpha = 10°$, $\beta = 18°$ at $s = 0.050$. The lowest part (a) shows the first-order incident wave, (b) shows the first-order incident and reflected waves; (c) and (d) show the incident and reflected waves at second and third order respectively.

scattered in z-wavenumber, whilst the motion continues to be periodic in time and in the coordinate parallel to the slope. The labour (and possibility of error) in extending the calculation algebraically to higher orders is daunting, and we have not attempted it, being content in this study to illustrate the major features which result from finite amplitude.

Figure 7 is an example of waves produced when $\alpha = 10°$, $\beta = 18°$ and $s = 0.050$, and is typical of the results obtained. Although the general features of the linear solution can still be detected as s increases, steep waves develop in local regions at some distance remote from the slope.

Figure 8 shows the 'critical' steepness, $s = s_c$, of the incident wave at which the slope of isopycnal surfaces calculated to first, second, and third orders first becomes vertical somewhere in the fluid, and beyond which the theory predicts that regions of static instability will develop. We do not claim that these estimates provide accurate predictions of the onset of static (and certainly not dynamic) instability although it is worth recalling that the onset of static instability in the (exact solution) first-order incident wave can be found exactly (equation (6)). Their value is rather to establish, as we shall see, the rather slow rates of convergence and to illustrate the range of variation. (We might equally well have taken some other, less severe,

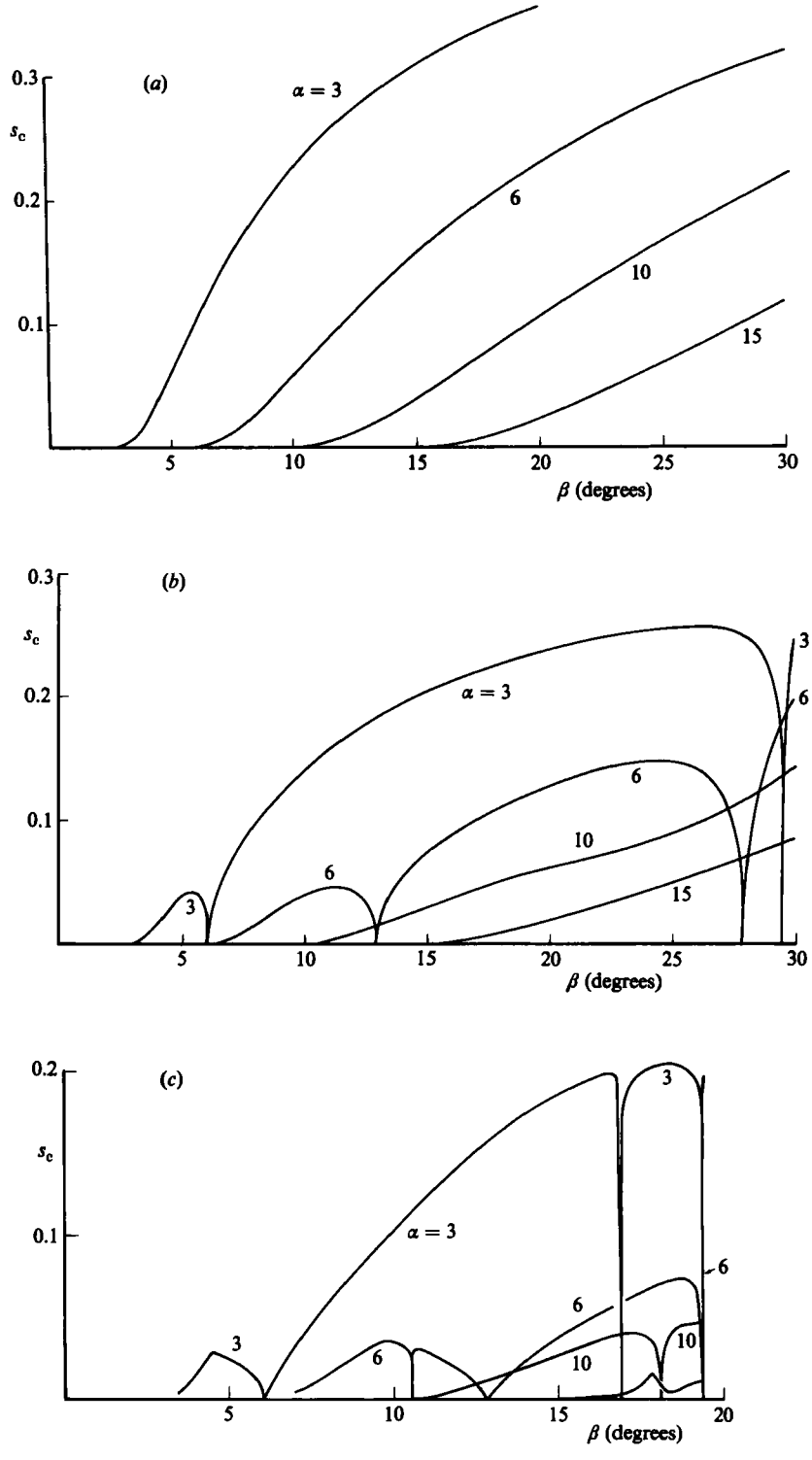

FIGURE 8. For caption see facing page.

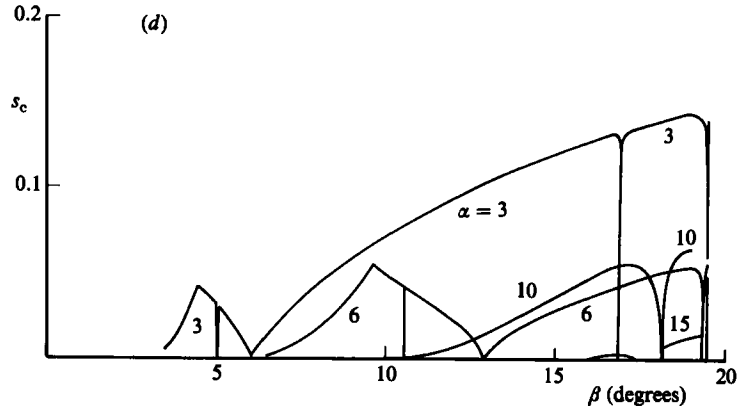

FIGURE 8. The steepness of the incident first-order waves s_c at which isopycnals first become vertical somewhere in the fluid at various values of α (specified on each curve in degrees) as β varies. (*a*) First-order waves, $\alpha < \beta \leqslant 30°$, (*b*) second order, $\alpha < \beta \leqslant 30°$, (*c*) third order $\alpha < \beta < 19.47°$. (*d*) The corresponding steepness of the incident wave calculated to third order.

criteria; see later.) The features resembling downward-pointing cusps appearing in figure 8 at second and third orders where, according to the calculations, s decreases towards zero, are at values of β where resonance occurs and where the solutions become invalid. The width of the band of incident-wave directions β affected by the *second-order* resonances (figure 8*b*) is about 1° at $\alpha = 3°$ and 1.5° at $\alpha = 6°$ at second order (figure 8*b*), but somewhat broader at third order (figure 8*c*). The predicted β-width at third-order resonance is much less, typically 0.2°. In figure 8(*d*) is shown the steepness s_c' of the incoming (k, n_I, σ) wave which now includes the third-order modification (equation (24)). For some values of α, β (for example $\alpha = 3°$, $4° < \beta < 5°$) $s_c' > x_c$ and s_c' is closer to the second-order value of s_c (figure 5*b*); here the third-order effects are less severe than suggested by s_c, but in general the converse is true. The decreasing β-width at resonances as the order of the expansion increases suggests that, although the number of possible 'resonances' increases as the order of the expansion increases, their width decreases in such a way that bounded solutions may be found over most of the (α, β, s)-domain but this should be re-examined in a more comprehensive theory. For $\alpha = 15°$ and $\beta \sim 17.8°$, the condition (26) is almost satisfied and n_{I3} becomes of magnitude comparable with n_{I1}, so that the incident slope become ill-defined to third order.

The effect of increasing order is to reduce the critical steepness significantly, demonstrating the influence of finite-amplitude effects (although providing no plausible demonstration of rapid convergence!). Such a test of the effects of finite amplitude is however extreme. In figure 9 we have instead displayed the value of s at which the sum of the second- and third-order contributions to the wave steepness become equal to a tenth of those contributed by the first-order terms. This shows that finite-amplitude effects become significant *even when the incident-wave steepness is quite small.* Figure 10 shows the modulus of the ratio of third-order to second-order terms r for the same value of s. Although generally less than unity, large values are found in the vicinity of the resonant singularities, and here it appears that, even at small slopes, additional terms may be required to provide reliable predictions near such points. The abrupt jumps in s and r (e.g. those bordering the second-order resonances at $\alpha = 3°$ and 6°) in figures 9 and 10 are due to an interchange between

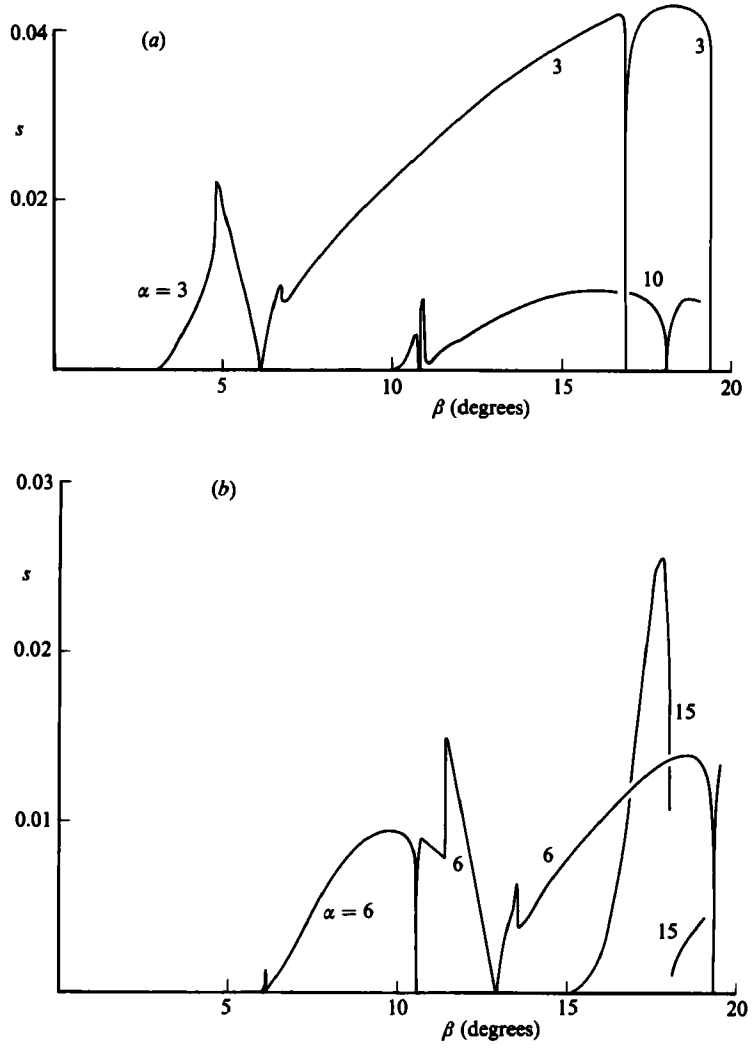

FIGURE 9. The steepness of the incident first-order wave s at which the sums of the second- and third-order contributions to the maximum wave steepness became equal to 0.1 times those contributed by first-order terms at various values of α: (*a*) $\alpha = 3°$, 10°, (*b*) $\alpha = 6°$, 15°, plotted as functions of $\beta (< 19.47°)$.

the two possible roots of the quadratic equation implied by the condition that the contributions of the second- and third-order terms to the wave steepness be a tenth of that of the first order.

There is another, more subtle, effect near resonance points. Since the velocity normal to the slope is zero at $z = 0$, the solutions for ψ which correspond to forced waves are matched by free waves and, as resonance is approached, these have not only equal large magnitude, and phase and along-slope wavenumbers, but almost equal slope. Hence the distance z before they become out of phase and at which their individual contributions to the wave slope become significant, *increases* as resonance is approached. The reduction in s near resonance shown in figure 9 is thus generally achieved at the expense of increasing the distance from the slope at which local conditions of static instability are likely to occur.

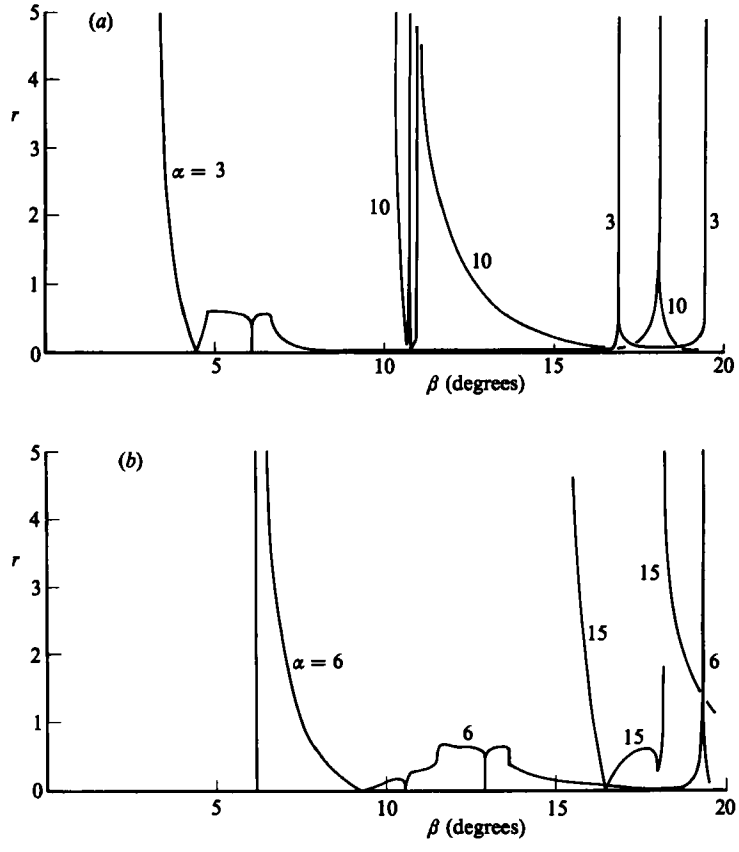

FIGURE 10. The modulus of the contributions to the wave steepness from third-order terms divided by those of second-order terms, r, in the same conditions as in figure 9.

4. Summary, and reflection at ocean boundaries

The effect of finite amplitude is to reduce the slope of the incident wave at which static (or dynamic) instability is probable, particularly in regions of the (α, β)-domain where resonance occurs, to distribute energy more widely in wavenumbers normal to the boundary, and to promote local static instability in regions remote from the boundary. In laboratory experiments (see Appendix C) instabilities are also found very close to the boundary slope which appear to differ from those reported by Cacchione & Wunsch (1974).

The effect of resonance on internal waves is well known (e.g. Martin, Simmons & Wunsch 1972; McEwan 1971; McEwan, Mander & Smith 1972). It is remarkable that the low-order conditions of resonance between incident and reflected waves shown in figures 2, 4–6 and 11, where nonlinear effects are likely to be most significant, occur only for low bottom slopes α – the conditions most common in the ocean – and at modest values of β where the oceanic internal-wave field is most energetic (i.e. at low frequencies). In the ocean the effect of resonance will be modified by the efficiency of reflection at the boundary (it may for example be affected by the reduced density gradients and by enhanced levels of turbulence in the benthic boundary layer, especially when the incident or reflected wavelengths normal to the boundary become

comparable with the boundary-layer thickness) and the magnitude to which the effects of resonance may grow will be limited by the non-stationary character of the internal-wave field. Account must be taken of the interaction between the primary incident wave, its reflected components and other waves present. The possibility of resonance will be modified by the effects of the Earth's rotation which introduces the additional parameter, f/N_0. (An effect of rotation is shown in figure 2 and 11*b*; it reduces the range of angles α and β at which resonance can occur.) Bottom roughness may require study, especially when the wavelength of the roughness is comparable with that of the waves (Baines 1971; Mied & Dugen 1976). The effect on resonance of viscosity and three-dimensionality (see Eriksen 1982, and Appendix B for further discussion) must be taken into account. Since, however, the root-mean-square internal-wave steepness estimated following the procedure described by Garrett & Munk (1972) is about 0.06, the results (e.g. figure 8) lend support to Eriksen's conclusion that conditions favouring internal-wave breaking will frequently occur near sloping ocean boundaries.

I am grateful to Dr Howell Peregrine for a remark which helped to clarify the interpretation of wave interaction at third order.

Appendix A. Second- and third-order solutions

Second-order solution

The stream function is

$$\psi_2 = B[s_* - \sin(2kx + (n_\mathrm{I}+n_\mathrm{R})z - 2\sigma t)] - \frac{a^2k^2}{\sigma\gamma} s_\beta c_\beta \sin(n_\mathrm{I}-n_\mathrm{R})z,$$

where
$$B = \frac{3a^2k^2 s_\beta^2 c_\beta^2 s_\alpha c_\alpha}{\sigma\gamma D}, \quad D = 4s_\beta^4 - 7s_\beta^2 s_\alpha^2 + 4s_\alpha^2 - s_\beta^2,$$

and
$$s_* = \begin{cases} \sin(2kx + m_2 z - 2\sigma t, & 2\sigma \leqslant N_0, \\ \mathrm{e}^{-m_\mathrm{r} z} \sin(2kx + m_\mathrm{i} z - 2\sigma t), & 2\sigma > N_0, \end{cases}$$

where $m_\mathrm{r} = 4k\sigma(4\sigma^2 - N_0^2)^{\frac{1}{2}}/(4\sigma^2 - N_0^2 s_\alpha^2)$, and $m_\mathrm{i} = -2kN_0^2 s_\alpha c_\alpha/(4\sigma^2 - N_0^2 s_\alpha^2)$. The curve $D = 0$ gives the condition for resonant interaction and is shown in figure 2. The normalized density is

$$\rho_2 = -\left(\frac{2a^2k^3 s_\alpha c_\beta^2}{g\gamma^2 D}\right)(2s_\beta^4 - 5s_\alpha^2 s_\beta^2 + 2s_\alpha^2 + s_\beta^2)\sin(2kx + (n_\mathrm{I}+n_\mathrm{R})z - 2\sigma t)$$

$$- \frac{2a^2k^3}{g\gamma^2} c_\alpha s_\beta c_\beta \sin(n_\mathrm{i} - n_\mathrm{R})z$$

$$+ \begin{cases} \dfrac{\sigma B}{2gs_\beta^2}(2kc_\alpha - m_2 s_\alpha)\sin(2kx + m_2 z - 2\sigma t), & 2\sigma \leqslant N_0, \\ -\dfrac{2B}{g} m_\mathrm{i}\, \mathrm{e}^{-m_\mathrm{r} z}[2\sigma s_\alpha \sin(2kx + m_\mathrm{i} z - 2\sigma t) \\ \quad + c_\alpha(4\sigma^2 - N_0^2)^{\frac{1}{2}} \cos(2kx + m_\mathrm{i} z - 2\sigma t)], & 2\sigma > N_0. \end{cases}$$

The mean Eulerian current parallel to the boundary is thus

$$\bar{u} = \frac{\overline{\partial\psi_2}}{\partial z} = -\frac{a^2k^2}{\sigma\gamma} s_\beta c_\beta (n_\mathrm{I} - n_\mathrm{R}) \cos(n_\mathrm{I} - n_\mathrm{R})z,$$

which can be written

$$\bar{u} = -\frac{A^2 k\sigma c_\beta^2 (\cos 2\alpha - \cos 2\beta)}{s_\beta \sin^3(\beta-\alpha)} \cos\left(\frac{2ns_\beta z}{\sin(\beta-\alpha)}\right),$$

where (k, n) are the horizontal and vertical incident wavenumbers and A is the incident-wave amplitude. This is unchanged in a rotating system. An incident internal wave thus drives an Eulerian off-slope flow at $z = 0$.

It may similarly be shown that the set-up of isopycnal surfaces is

$$\bar{\zeta}_2 = -\frac{A^2 k (\cos 2\alpha - \cos 2\beta) c_\alpha c_\beta}{2 \sin^3(\beta-\alpha)} \sin\left(\frac{2ns_\beta z}{\sin(\beta-\alpha)}\right)$$

and the apparent up-slope density flux (neglecting that carried by the Eulerian current) is

$$F = -\frac{A^2\sigma}{2}\frac{N_0^2}{g}\rho_0 \frac{c_\alpha c_\beta (\cos 2\alpha - \cos 2\beta)}{s_\beta \sin^2(\beta-\alpha)} \sin\left(\frac{2ns_\beta z}{\sin(\beta-\alpha)}\right).$$

Third-order solution; $\beta \leqslant \sin^{-1}(\frac{1}{3})$

The coefficients of terms for the stream funcion ψ_3 are as follows:

$$[\sin(3kx + (2n_I + n_R)z - 3\sigma t) - \sin(3kx + m_3 z - 3\sigma t)] :- \frac{A_1(B_2 - B_3)}{\mathscr{F}(3k, 2n_I + n_R, 3\sigma)},$$

where

$$A_1 = \frac{2a^3k^5(n_R - n_I)s_\alpha c_\beta^2 s_\beta}{\gamma D},$$

$$B_2 = 3c_\alpha s_\beta(4s_\beta^4 - 6s_\alpha^2 s_\beta^2 - 3s_\alpha^2 - s_\beta^2),$$

$$B_3 = c_\beta s_\alpha(s_\beta^4 + 5s_\alpha^2 s_\beta^2 + s_\alpha^2 - 7s_\beta^2);$$

$$[\sin(3kx + (2n_R + n_I)z - 3\sigma t) - \sin(3k + m_3 z - 3\sigma t)] :- \frac{A_1(B_2 + B_3)}{\mathscr{F}(3k, 2n_R + n_I, 3\sigma)},$$

$$[\sin(kx + (2n_I - n_R)z - \sigma t) - \sin(kx + n_R z - \sigma t)] :- \frac{A_2}{\mathscr{F}(k, 2n_I - n_R, \sigma)},$$

where

$$A_2 = \frac{2a^3k^5(n_R - n_I)s_\beta c_\beta^3}{\gamma^2}.$$

$$[\sin(kx + (2n_R - n_I)z - \sigma t) - \sin(kx + n_R z - \sigma t)] :- \frac{-A_2}{\mathscr{F}(k, 2n_R - n_I, \sigma)},$$

$$[\sin(3kx + (n_I + m_2)z - 3\sigma t) - \sin(3kx + m_3 z - 3\sigma t)] :-$$

$$\frac{ak\sigma B(2n_I - m_2)[6(n_I^2 - 3k^2 - m_2^2) - (2n_I - m_2)(3kc_\alpha - (n_I + m_2)s_\alpha)/s_\beta^2]}{4\mathscr{F}(3k, n_I + m_2, 3\sigma)},$$

$$[\sin(3kx + (n_R + m_2)z - 3\sigma t) - \sin(3kx + m_3 z - 3\sigma t)] :-$$

$$\frac{ak\sigma B(2n_R - m_2)[6(m_2^2 + 3k^2 - n_R^2) + (2n_R - m_2)(3kc_\alpha - (n_R + m_2)s_\alpha)/s_\beta^2]}{4\mathscr{F}(3k, n_R + m_2, 3\sigma)},$$

$$[\sin(kx + (m_2 - n_I)z - \sigma t) - \sin(kx - n_R z - \sigma t)] :-$$

$$\frac{ak\sigma B(2n_I - m_2)[2(m_2^2 + 3k^2 - n_I^2) + (2n_I - m_2)(kc_\alpha - (m_2 - n_I)s_\alpha)/s_\beta^2]}{4\mathscr{F}(k, m_2 - n_I, \sigma)},$$

$$[\sin(kx+(m_2-n_R)z-\sigma t)-\sin(kx+n_R z-\sigma t)]:-$$

$$\frac{ak\sigma B(2n_R-m_2)[2(n_R^2-3k^2-m_2^2)-(2n_R-m_2)(kc_\alpha-(m_2-n_R)s_\alpha)/s_\beta^2]}{4\mathscr{F}(k,m_2-n_R,\sigma)}.$$

The corresponding terms for ρ_3 can be found by multiplying terms in ψ_3 by $N_0^2(c_\alpha k_i - s_\alpha n_i)/(g\sigma_i)$, where k_i, n_i, σ_i are the appropriate vector number and frequency, and adding the following terms

$$\frac{akN_0^2}{2g\sigma}\Bigg\{\left[(P_1-P_2)-\left(\frac{B+C}{\sigma}\right)(kc_\alpha-n_R s_\alpha)\right](n_R-n_I)\sin(kx+n_I z-\sigma t)$$

$$+\left[(P_1+P_2)-\left(\frac{B-C}{\sigma}\right)(kc_\alpha-n_I s_\alpha)\right](n_R-n_I)\sin(kx+n_R z-\sigma t)$$

$$+\left(\frac{n_I-n_R}{3}\right)\left[P_1-\frac{B}{\sigma}(kc_\alpha-n_I s_\alpha)\right]\sin(3kx+(2n_I+n_R)z-3\sigma t)$$

$$+\left(\frac{n_I-n_R}{3}\right)\left[P_1-\frac{B}{\sigma}(kc_\alpha-n_R s_\alpha)\right]\sin(3kx+(2n_R+n_I)z-3\sigma t)$$

$$-(n_I-n_R)\left[P_2+\frac{C}{\sigma}(kc_\alpha-n_I s_\alpha)\right]\sin(kx+(2n_I-n_R)z-\sigma t)$$

$$+(n_I-n_R)\left[P_2+\frac{C}{\sigma}(kc_\alpha-n_R s_\alpha)\right]\sin(kx+(2n_R-n_I)z-\sigma t)$$

$$-\frac{B}{6\sigma}s_\alpha(2n_I-m_2)^2\sin(3kx+(n_I+m_2)z-3\sigma t)$$

$$+\frac{B}{6\sigma}s_\alpha(2n_R-m_2)^2\sin(3kx+(n_R+m_2)z-3\sigma t)$$

$$+\frac{B}{2\sigma}s_\alpha(2n_I-m_2)^2\sin(kx+(m_2-n_I)z-\sigma t)$$

$$-\frac{B}{2\sigma}s_\alpha(2n_R-m_2)^2\sin(kx+(m_2-n_R)z-\sigma t)\Bigg\},$$

where

$$P_1=\frac{2a^2k^3s_\alpha}{N_0^2\gamma^2 D}c_\beta^2(2s_\beta^4-5s_\alpha^2 s_\beta^2+2s_\alpha^2+s_\beta^2),$$

$$P_2=-\frac{2a^2k^3c_\alpha s_\beta c_\beta}{N_0^2\gamma^2}$$

$$C=\frac{a^2k^2s_\beta c_\beta}{\sigma\gamma}.$$

Appendix B. Conditions for resonance at second order in more general conditions

We consider the conditions for reflection of a plane wave which is not propagating in a vertical plane normal to the line of greatest slope (i.e. the axis x' of figure 1). If now the wavenumber in a direction normal to the axes (x', z') in figure 1 is l and,

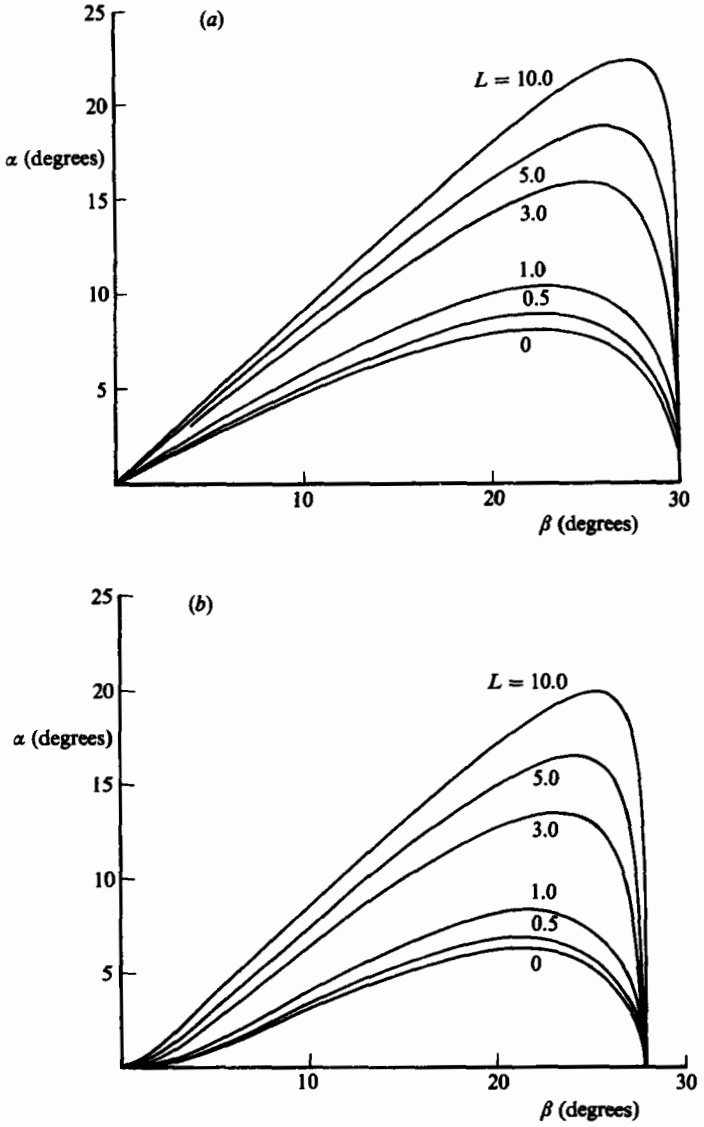

FIGURE 11. The loci of points in the (α, β)-plane where conditions of resonance are found at second order when the along-slope wavenumber l can be non-zero. Values of $L = l/k$ are given on each curve: (*a*) $f/N_0 = 0$; (*b*) $f/N_0 = 0.2$.

as before, k and n are the wavenumbers in directions x' and z', then the dispersion relation becomes

$$\sigma^2 = \frac{N_0^2[(kc_\alpha - ns_\alpha)^2 + l^2]}{(k^2 + l^2 + n^2)}.$$

On reflection the wavenumbers k and l and the frequency σ are conserved and the z' wavenumbers are found by solving the dispersion relation. Their sum is $n_I + n_R = -2s_\alpha c_\alpha/(s_\beta^2 - \sigma_\alpha^2)$, where $s_\beta = \sigma/N_0$, and is independent of l. For resonance

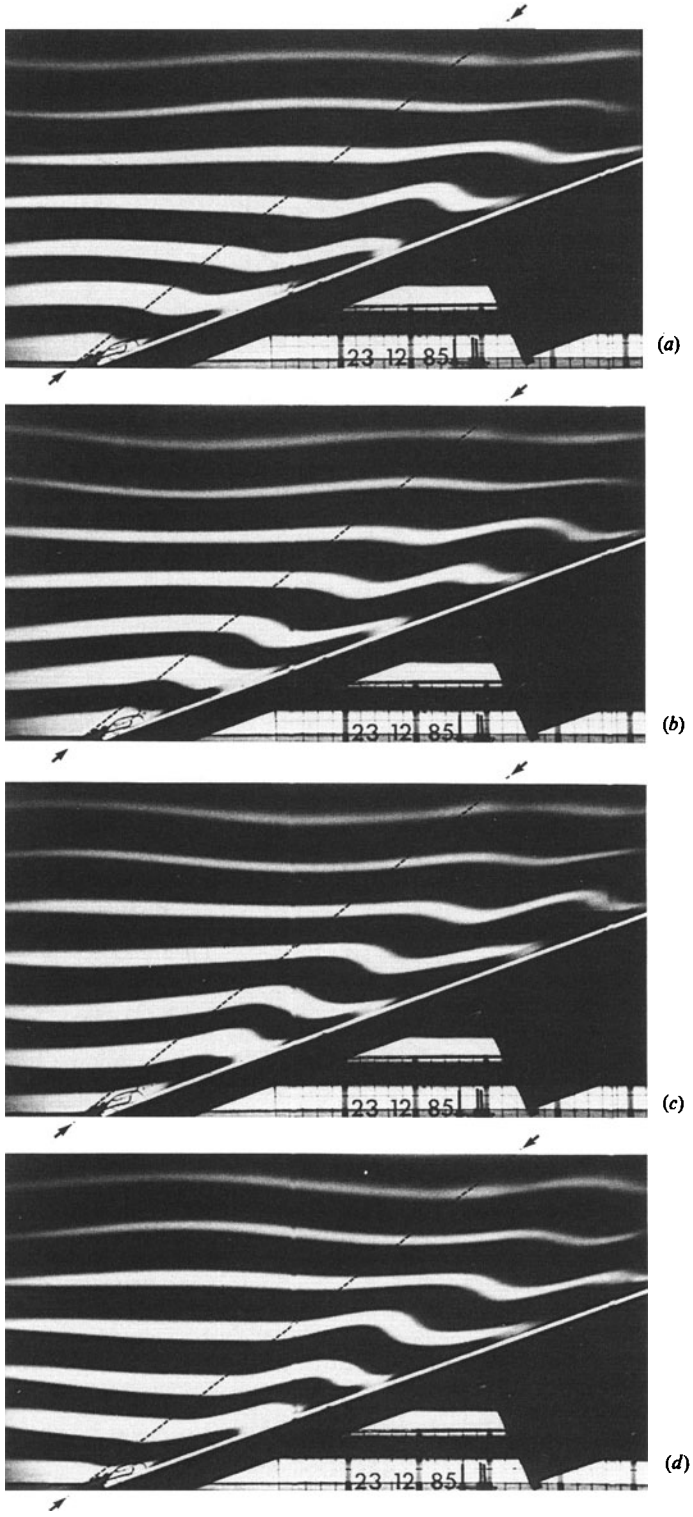

FIGURE 12. Wave reflection from a beach, $\alpha = 20°$, $\beta = 37.9°$ and $s = 0.07$. The incident wave of the second vertical mode can be seen approaching the beach at the left. Reflection from the downward-going component occurs below the dashed line. The four photographs are at one-quarter-period intervals. The grid below the beach shows 1 cm squares. The bottom of the laboratory tank is at the bottom of each photograph, and the free surface of the water is 3.7 cm above the top of each photograph.

at second order, the wave of wavenumber vector $(2k, 2l, n_I+n_R)$ and frequency 2σ must satisfy the dispersion relation. This is so if

$$D \equiv 4s_\beta^4 - 7s_\beta^2 s_\alpha^2 + 4s_\alpha^2 - s_\beta^2 = \frac{L^2}{s_\beta^2}(s_\beta^2 - s_\alpha^2)^2(1-4s_\beta^2),$$

where $L = l/k$. The values of α and β at which this condition is satisfied are shown in figure 11 (*a*) for various values of L.

The effect of non-zero l is to increase the values of $\alpha(<\beta)$ at which resonance, and hence strong nonlinear effects, may occur. (An additional branch of the (α, β)-curve is found for $\alpha > \beta$, but this case has been specifically excluded from the present discussion.) Resonant values are found only for $\beta < 30°$. In the limit as L tends to infinity, the resonance curves tend towards $\alpha = \beta$ and $\beta = 30°$.

If, in addition, the fluid is rotating we have $s_\beta^2 = (\sigma^2 - f^2)/(N_0^2 - f^2)$ and the dispersion relation is

$$\sigma^2 = \frac{N_0[(kc_\alpha - ns_\alpha)^2 + l^2] + f^2(ks_\alpha + nc_\alpha)^2}{k^2 + l^2 + n^2}.$$

The conditions of second-order resonance can again be found. Those for $L \equiv l/k = 0$ are shown in figure 2. The conditions for resonance at $f/N_0 = 0.2$ at various L are given in figure 11 (*b*). The effect here of rotation is to diminish the ranges of α and β at which resonance occurs.

Appendix C.

A note on observations of wave reflection on a 20° slope

By S. A. Thorpe and A. P. Haines

We have made laboratory experiments in which progressive internal waves of the second vertical mode, generated in a saline fluid of constant density gradient, are incident on a uniform sheet of glass forming a slope inclined to the horizontal at $\alpha = 20°$. Earlier experiments by Thorpe (see Turner 1973), Wunsch (1969) and Cacchione & Wunsch (1974) have demonstrated how the wave amplitude changes on reflection. The latter authors demonstrated the occurrence of an instability manifest as a series of vortices with horizontal axes in the boundary layer adjoining the slope at the critical frequency when $\alpha = \beta$.

Figure 12 shows reflection occurring at $\beta = 37.9°$. The incident-wave displacements $\zeta = a_0 \cos(kx - \sigma t) \sin n_I z$, where $n_I = 2\pi/h$ and h is the channel depth (27.9 cm), can be expressed as the sum of upward- and downward-going waves, $\zeta = \frac{1}{2}a_0[\sin(kx + n_I z - \sigma t) - \sin(kx - n_I z - \sigma t)]$, each travelling at angle β to the horizontal and of half the amplitude of the second mode. In the figure the incident second-mode wave can be seen to the left producing displacements in dye bands. Within the triangle formed between the slope and the dashed line drawn from the foot of the slope can be seen the combined downward-going part of ζ and its reflection; geometrically, the upward-going part of the incident wave cannot reach this area. The form and slopes of the waves are in fair agreement with the theoretical estimate shown for the same values of s, α and β in figure 3; the efficiency of reflection appears to be large.

Wave overturn, when it occurs, generally appears to be well above the beach and is on the same scale as the reflected waves, suggesting locally generated conditions of static instability rather than a shear flow, or Kelvin–Helmholtz, instability on a

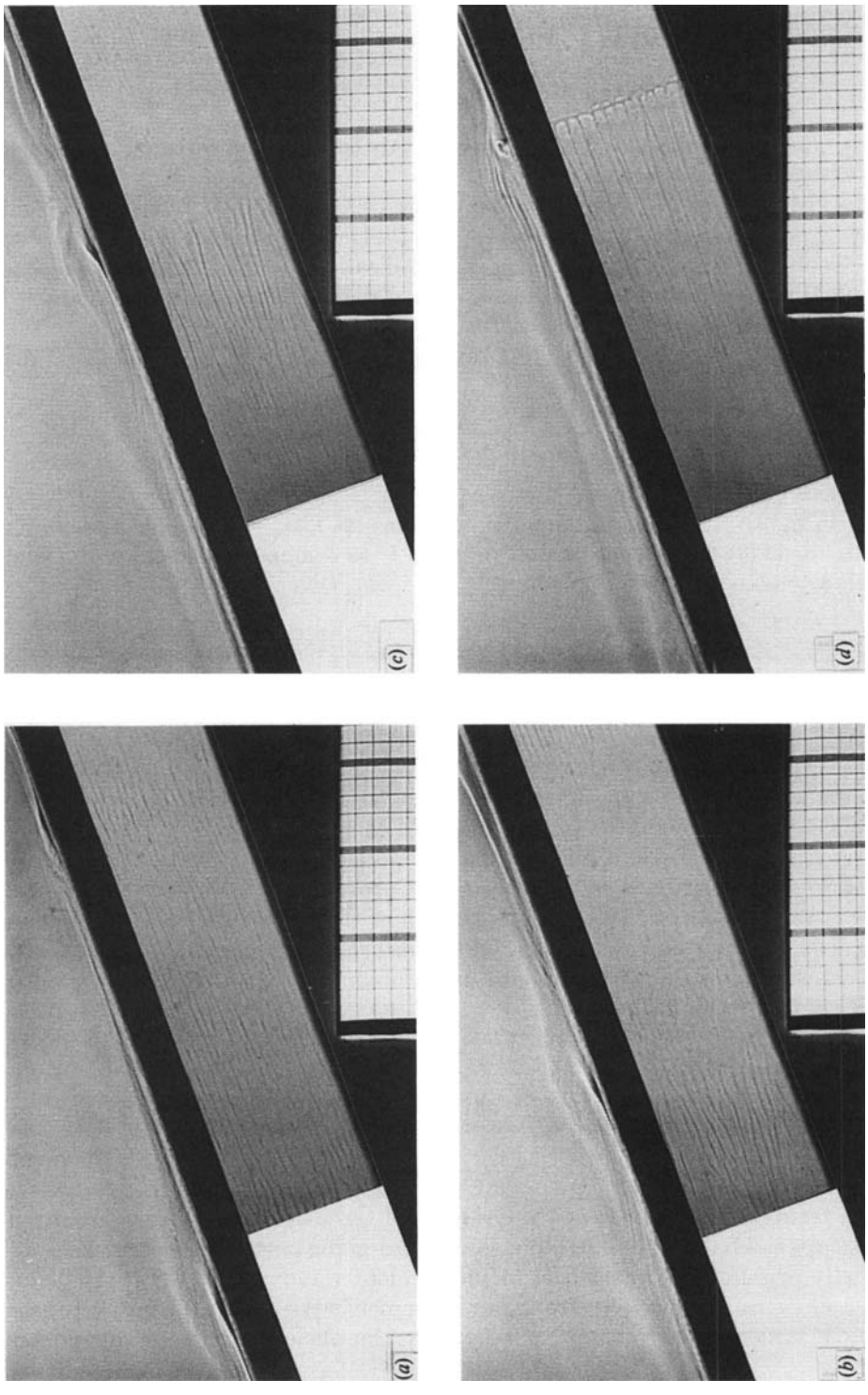

FIGURE 13. Shadowgraph images showing the side (above the slope) and plan (below the slope) views of waves at the beach with $\alpha = 20°$, $\beta = 21.1°$ and $s = 0.03$. The four photographs are at one-quarter-period intervals. The grid below the beach shows 1 cm squares. In the plan view strips 3.8 cm wide are masked at each side of the tank so that the image does not extend to the sidewalls. The mid-depth of the fluid lies 9.0 cm above the top of the grid.

scale determined by local shear. We would however caution that the Reynolds number of the waves in the experiments is not large (i.e. $a_0^2\sigma/\nu \sim 20$, where ν is the kinematic viscosity) and may not be sufficient to permit the development of a shear-flow instability.

Although little energy appears to be lost on reflection, effects *are* seen in the boundary layer on the slope. Figure 13 shows a shadowgraph produced by shining a parallel beam of light horizontally through the side of the tank (producing the part of the image above the slope), and vertically down through the glass slope via a 45° mirror onto a screen on the side of the tank (producing the 'planform' image below the slope). Although the interpretation of images produced by shadowgraph is sometimes ambiguous, it is apparent that 'fronts' are produced with a left-and-lobe structure similar to that described by Simpson (1972), together with a pattern of bands aligned up and down the slope, when motion is directed up-slope; the boundary layer has a three-dimensional structure. This probably results from the action of viscosity in promoting regions of static instability in a narrow shear layer as fluid is moved up-slope by the wave motion, advecting dense fluid over the more slowly moving fluid near the slope. Up-slope-going motions are thus likely to produce more boundary mixing than the down-slope motions. The 'fronts' appear to result in part from convergent motion in a direction up the slope, a feature perhaps amplified by the presence of the second mode, but absent (or virtually so) from the related experiments by Hart (1971) in which an inclined plane was oscillated in its own plain in a stratified fluid. The vortices reported by Cacchione & Wunsch in their study of a first-mode incident wave on a 15° slope have not been found in the present experiments.

REFERENCES

Baines, P. G. 1971 The reflexion of internal/inertial waves from bumpy surfaces. *J. Fluid Mech.* **46**, 273–291.

Cacchione, D. & Wunsch, C. 1974 Experimental study of internal waves over a slope. *J. Fluid Mech.* **66**, 223–240.

Eriksen, C. C. 1982 Observations of internal wave reflection off sloping bottoms. *J. Geophys. Res.* **87**, 525–538.

Eriksen, C. C. 1985 Implications of ocean bottom reflection for internal wave spectra and mixing. *J. Phys. Oceanogr.* **15**, 1145–1156.

Garrett, C. 1979 Mixing in the ocean interior. *Dyn. Atmos. Oceans*, **3**, 239–265.

Garrett, C. & Munk, W. 1972 Oceanic mixing by breaking internal waves. *Deep-Sea Res.* **19**, 823–832.

Görtler, H. 1943 Uber eine Schwingungerscheinung in Flussigkeiten mit stabiler Dichteschichtung. *Z. Angew. Math. Mech.* **23**, 65–71.

Hart, J. E. 1971 A possible mechanism for boundary layer mixing and layer formation in a stratified fluid. *J. Phys. Oceanogr.* **1**, 258–262.

McEwan, A. D. 1971 Degeneration of resonantly-excited standing internal gravity waves. *J. Fluid Mech.* **50**, 431–448.

McEwan, A. D., Mander, D. W. & Smith, R. K. 1972 Forced resonant second-order interaction between damped internal waves. *J. Fluid Mech.* **53**, 589–608.

Martin, S., Simmons, W. F. & Wunsch, C. I. 1972 The excitation of resonant triads by single internal waves. *J. Fluid Mech.* **53**, 17–44.

Mied, R. P. 1976 The occurrence of parametric instability in finite-amplitude internal gravity waves. *J. Fluid Mech.* **78**, 763–784.

Mied, R. P. & Dugan, J. P. 1976 Internal wave reflexion from a sinusoidally corrugated surface. *J. Fluid Mech.* **76**, 259–272.

MOWBRAY, D. E. & RARITY, B. S. H. 1967 A theoretical and experimental investigation of internal waves of small amplitude in a density stratified liquid. *J. Fluid Mech.* **28**, 1–16.

MUNK, W. H. 1966 Abyssal recipes. *Deep-Sea Res.* **13**, 207–230.

PHILLIPS, O. M. 1966 *The Dynamics of the Upper Ocean.* Cambridge University Press. 261 pp.

PHILLIPS, O. M. 1970 On flows induced by diffusion in a stably stratified fluid. *Deep-Sea Res.* **17**, 435–443.

SIMPSON, J. E. 1972 Effects of the lower boundary on the head of a gravity current. *J. Fluid Mech.* **53**, 759–768.

THORPE, S. A. 1968 On the shape of progressive internal waves. *Phil. Trans. R. Soc. Lond.* A**263**, 563–614.

THORPE, S. A. 1978 On internal gravity waves in an accelerating shear flow. *J. Fluid Mech.* **88**, 623–639.

THORPE, S. A. 1982 On the layers produced by rapidly oscillating a vertical grid in a uniformly stratified fluid. *J. Fluid Mech.* **124**, 391–409.

THORPE, S. A. 1987 Transitional phenomena and the development of turbulence in stratified fluids: a review. *J. Geophys. Res.* (to appear).

TURNER, J. S. 1973 *Buoyancy Effects in Fluids.* Cambridge University Press. 367 pp.

WUNSCH, C. 1969 Progressive internal waves on slopes. *J. Fluid Mech.* **35**, 131–144.

WUNSCH, C. 1970 On oceanic boundary mixing. *Deep-Sea Res.* **17**, 293–301.

WUNSCH, C. 1971 Note on some Reynolds stress effects of internal waves on slopes. *Deep-Sea Res.* **18**, 583–591.